ACKNOWLEDGMENT

The authors wish to acknowledge the helpful consultation of Professor R. R. Hughes at the University of Wisconsin. This work was supported by the Wisconsin Alumni Research Foundation, the University of Wisconsin Graduate School and Chemical Engineering Department, the National Science Foundation, and the Oak Ridge National Laboratory, which is operated by Union Carbide Corporation for the Department of Energy.

NOTATION

CAP_j = capital investment required for j^{th} tower (see Tedder, 1975)
d_j = observed deviation in rank order between the predicted rank and the observed rank
I_{Xj} = observed rank order for j^{th} tower
I_{Yj} = predicted rank order for j^{th} tower
N_j = minimum theoretical stages for j^{th} tower calculated from Fenske equation (see Part III)
OP_j = annual operating costs for j^{th} tower (see Tedder, 1975)
P = optimal overhead operating pressure, MN/m^2
R_s = spearman rank correlation coefficient
T = tower feed normal bubble point, °K
VC = annual venture cost (see Tedder, 1975)
V_j^U = minimum vapor requirements for j^{th} tower as calculated by the Underwood equation (see Part III)
X_j = observed minimum venture cost for j^{th} tower
Y_j = predicted minimum venture cost for j^{th} tower, minus the least-squares regression constant for models 2, 3, 4, 5, and 6 in Table 1, or divided by the multiplication constant for models 1, 7, 8, and 10.
δT_j = temperature drop up the j^{th} tower

LITERATURE CITED

Aris, R. *The Optimal Design of Chemical Reactors,* Academic Press, New York (1961).

Bellman, R. E., *Dynamic Programming,* Princeton Univ. Press, N.J. (1957).

Beveridge, G. S. C., and R. S. Schechter, *Optimization: Theory and Practice,* McGraw-Hill, New York (1970).

Brosilow, C., and L. S. Lasdon, "Two-Level Optimization Techniques for Recycle Processes," *Proc. Symp. No. 4,* 67, AIChE—I. Chem. E. Joint Meeting (1965).

Freshwater, D. C., and B. D. Henry, "Optimal Configuration of Multicomponent Distillation Systems," paper presented at AIChE National Meeting, Tulsa, Okla. (Mar. 10-13, 1974).

Harbart, W. D., "Which Tower Goes Where?," *Petrol Refiner,* 36, 169 (1957).

Hendry, J. E., "Computer Aided Synthesis of Optimal Multicomponent Separation Sequences," Ph.D. thesis, Univ. Wisc., Madison (1972).

———, and R. R. Hughes, "Generating Separation Process Flowsheets," *Chem. Eng. Progr.,* 68, No. 6, 69 (1972).

Ichikawa, A., and L. T. Fan, "Optimal Synthesis of Process Systems, Necessary Condition for Optimal System and its use in Synthesis of Systems," *Chem. Eng. Sci.,* 28, 357 (1973).

Lockhart, F. J., "Multi-Column Distillation of Natural Gasoline," *Petrol. Refiner,* 26, 104 (1947).

Masso, A. H., and D. F. Rudd, "The Synthesis of System Designs II Heuristic Structuring," *AIChE J.,* 15, No. 1, 10 (Jan., 1969).

Mendenhall, W., and R. L. Scheaffer, *Mathematical Statistics with Applications,* Duxbury Press, North Scituate, Mass. (1973).

McCabe, W. L., and J. C. Smith, *Unit Operations of Chemical Engineering,* McGraw-Hill, New York (1967).

Powers, G. J., "Recognizing Patterns in the Synthesis of Chemical Processing Systems," Ph.D. thesis, Univ. Wisc., Madison (1971).

Rathore, R. N. S., K. A. Van Wormer, and G. J. Powers, "Synthesis Strategies for Multicomponent Separation Systems with Energy Integration," *AIChE J.,* 20, No. 3, 491 (May, 1974).

———, "Synthesis of Distillation Systems with Energy Integration," *ibid.,* No. 5, 940 (Sept., 1974).

Robinson, C. S., and E. R. Gilliland, *Elements of Fractional Distillation,* 4 ed., McGraw-Hill, New York (1950).

Rod, V., and J. Marek, "Separation Sequences in Multicomponent Rectification," *Coll. Czech. Chem. Comm.,* 24, 3240 (1959).

Rudd, D. F., "The Synthesis of System Designs: I Elementary Decomposition Theory," *AIChE J.,* 14, No. 2, 343 (Mar., 1968).

———, G. J. Powers, and J. J. Siirola, *Process Synthesis,* Prentice Hall, N.J. (1973).

Siirola, J. J., G. J. Powers, and D. F. Rudd, "Synthesis af System Designs, III: Toward a Process Concept Generator," *AIChE J.,* 17, 677 (1971).

Siirola, J. J., and D. F. Rudd, "Cpmputer-Aided Synthesis of Chemical Process Designs," *Ind. Eng. Chem. Fundamentals,* 10, 353 (1971).

Tazaki, E., A. Shindo, and T. Umeda, "Decentralized Optimization of a Chemical Process by a Feasible Method," *Automatica,* 8, 543 (1972).

Tedder, D. W., "The Heuristic Synthesis and Topology of Optimal Distillation Networks," Ph.D. thesis, Univ. Wisc., Madison (1975).

Thompson, R. W., and C. J. King, "Systematic Synthesis of Separation Schemes," *AIChE J., 18,* No. 5, 941 (Sept., 1972).

Umeda, T., A. Hirai, and A. Ichikawa, "Synthesis of Optimal Processing System by an Integrated Approach," *Chem. Eng. Sci.,* 27, 795 (1972).

Umeda, T., A. Shindo, and E. Tazaki, "Optimal Design of Chemical Process by Feasible Decomposition Method," *Ind. Eng. Chem. Process Design Develop.,* 11, No. 1, 1 (1972).

Manuscript received April 29, 1977; revision received ond accepted December 16, 1977.

Part III. Design Methods and Their Evaluation

Distillation networks are described as sets of composition nodes which are used to estimate material and energy balances. Comparisons with equivalent, equilibrium stage models indicate that these simplified design methods consistently result in small, but acceptable, overdesign, even when applied to complex, thermally coupled tower configurations.

SCOPE

The incentives for state optimizing various processing trains increase with rising capital and operating costs. When a process design analysis is based on countercurrent equilibrium stage models, then each evaluation of the economic objective function requires a prior numerical convergence to the underlying energy and material balances. It is possible to use such a model to perform design optimization as has been done by Ricker and Grens (1974), but this method becomes exceedingly burdensome when

Correspondence concerning this paper should be addressed to D. William Tedder, Oak Ridge National Laboratory, P. O. Box X, Oak Ridge, TN 37830.

the objective is to assess the economics of many design alternatives. Even when the calculations are performed on a high-speed computer, it is often not practical to evaluate hundreds or thousands of points on the economic response surface of many design alternatives, especially if each state point evaluation requires a minute or more CPU time to converge on the energy and material balances for each tower in the design. Realistically, it is necessary to evaluate each point on the design economic response surface in a one-tenth of a second or less.

Computational methods for distillation are presented which facilitate such rapid economic objective function evaluations. They are based on quickly estimating material balances via heuristic species allocation and a novel approach whereby a tower is considered to consist of a set of nonequilibrium stages or vertexes. At each stage, or composition node in the design model, countercurrent vapor and liquid streams are defined, each with the same composition. Vapor and liquid profiles in the tower are then defined in terms of combined overall energy and material balances, rather than assuming constant molal overflow. Since individual component balances are not involved in the intratower calculations, the need for referencing adjacent trays, and the numerical complexity of tridiagonal matrices, is avoided.

The topological representation of eight distillation networks, separating ternary mixtures, is presented (see Part 1). The composition node design method (CNDM) was used to provide the energy and material balance information required as input to the detailed economic models comparing these distillation alternatives. The validity of the CNDM is examined by arbitrarily comparing eight distillation towers which had been state optimized using the approximate method, with the material and energy balances which result by modeling these same towers as a set of equilibrium stages. The Thiele-Geddes method (see Newman, 1967) was used for these latter calculations.

CONCLUSIONS AND SIGNIFICANCE

The design methods described are useful tools for quickly estimating the energy and material balances associated with simple and complex distillation configurations. Comparisons with equivalent equilibrium stage models indicate that the approximations used in the design model tend to overestimate the utility requirements and give rather poor estimates of the feed tray composition. These design methods should not be used to infer the technical feasibility of a particular operating mode but rather to support detailed economic screening models for identifying attractive design configurations and their approximate optimal operating state. The design feasibility can then be verified with an equivalent equilibrium stage model simulating operation at the optimal state.

The CNDM normally overdesigns a tower by a small and acceptable amount. The overdesign is smaller for towers performing sharp cuts than it is for towers producing streams with distributed components. The overdesign is not proportional to tower size. Assumptions regarding contaminant concentrations in the product streams do not strongly affect the vapor estimates, but they can affect the minimum theoretical stage estimates and cause gross overestimation of the required tower height.

Composition node design models (CNDM) are approximate methods which estimate the essential design parameters needed to economically evaluate a collection of processing equipment items. They are useful in describing multistage countercurrent separation processes with the fewest possible trial and error calculations.

This simplified design method is derived from the classical Fenske-Underwood method, but it is faster because it eliminates much of the trial and error calculations usually required. In particular, with the classical method (see Robinson and Gilliland, 1950), the composition of product streams for a particular tower (the overall material balances) are recomputed for each change in the tower operating state which is considered. This computation is iterative in the classical method and is repeated during the operating state search to minimize costs. With the CNDM, the product material balances are computed by heuristic species allocation prior to the time at which the state optimization is initiated. The product compositions do not change during the optimization, and the trial and error calculations associated with the classical method are eliminated entirely. Some trial and error calculations are still required, for example, when estimating the feed tray composition (see PINCH algorithm in the appendix) or for certain product streams with distributed components (see DISTRIB algorithm in the appendix), but these calculations are relatively easy. In addition, trial and error calculations are still required to estimate the bubble- and dew-point temperatures associated with the various streams.

However, the composition of streams connecting towers are fixed prior to initiating the state optimization. So, interactions between towers, due to changes in material rates flowing between them, do not occur with the CNDM, whereas they would occur with the classical method. In addition, by heuristically assigning material balances using species allocation, all design alternatives have identical overall material balances. In contrast, evaluations based on either the classical Fenske-Underwood method or equilibrium stage models would give slightly different product compositions for each design configuration considered. However, this problem is avoided by using the CNDM.

The sequence of the economic design model computations is then as follows. First, the overall material balances are defined using a species allocation model (SAM). Then, an operating state is specified, and the CNDM is used to estimate the resulting energy and material balances for the tower under consideration. The tower may have any number of feeds and product streams and may be thermally coupled to other towers as well. At this point, it is then possible to carry out detailed sizing calculations to define all necessary equipment dimensions, etc., and to estimate the capital investment and annual

operating costs associated with each item. [The details of the sizing and cost models, which were used to generate venture cost information presented in Part I, are given elsewhere (Tedder, 1975)]. Based upon the resulting venture cost, the operating state of the tower is adjusted (but usually not the overall material balances), and the calculations are repeated, starting with the CNDM estimation of the internal molar vapor and overflow rates in the tower and the new energy balances. The resulting venture cost of the equipment assembly is then calculated and the state search terminated when a global minimum has been found.

NETWORK TOPOLOGIES

The topology of a tower is defined by that minimum set of composition vertexes needed to represent the design structure. A tower containing $k - 1$ sections, for example, can be described with k vertexes, each vertex being either a feed or product tray, where all vertex compositions and total pressures must be estimated in order to design the tower.

The aggregate of the individual towers without any interconnections between them is called the primitive system. A design can generally be defined in terms of the primitive system together with the tower interconnections and the original feed connection. Thus, the topology of any countercurrent separation network is determined by three factors:

1. The number of towers (or vertical paths) in the design.
2. The number of vertexes or nodes associated with each tower (or vertical path) in its primitive system representation.
3. The manner in which the interconnections (or horizontal paths) between the towers are made.

A network performing N splits can require more or less than $N - 1$ towers. Moreover, when a complex tower is permitted, the number of composition vertexes required to describe it can also vary, since there is a one-to-one correspondence between the vertexes and the number and location of product draws and feed trays for that tower. This variability gives rise to the need to classify each tower according to its structural type.

In general, structural type j contains $j + 1$ vertexes in its primitive system. It has an incidence matrix M_j, such that the top and bottom rows will contain only two nonzero elements. All intermediate rows have four nonzero elements. The dimensions of M_j are $j + 1$ by $2j$. A more detailed description is given elsewhere (Tedder, 1975).

The composition nodes defined within a network are of two types: internal or external. The internal nodes are those whose composition must change during the state optimization. The overhead and bottom product compositions in the upstream tower of design V are of this type, since the amount of separation work performed by the upstream tower is being optimized upon. Similarly, for all designs, the feed tray composition must also vary during the state optimization, since it is necessary to optimize the feed tray location and the number of stages above and below it.

The external vertexes are those nodes whose composition can be fixed by species allocation before the state optimization is initiated and which remain fixed throughout the optimization. The original feed compositions and the final product compositions can all be defined as external nodes within acyclic distillation trains. Moreover, when different designs are compared using this technique, they will all produce exactly the same products for a given feed.

Species Allocation Methods

The towers in a distillation network are connected by a set of intermediate feed and product streams. It is the object of the species allocation to specify the rates and compositions of these interconnecting links. This assignment is performed by synthesizing a species allocation composition (SAC) array with dimensions $2N - 1$ by N, where N components are separated. Estimates of the final product stream compositions are obtained from particular rows of the SAC array. This information is then used to define the interconnecting links.

The equations used in species allocation model No. 1 (SAM 1) to calculate the SAC array are shown in Table 1. This system of equations is solved iteratively after each row in the SAC array has been initially set equal to the original feed composition. The model is based upon the Fenske equation which is used in the following manner. Assume that a countercurrent tray exists whose liquid composition is equal to the composition of the external feed for ($X_{i,N}$, $i = 1, 2, , , N$) containing N components. Now, consider a set of trays located above the reference feed tray, row N in the SAC array. Each of these is separated by any number of minimum theoretical stages as defined by Equation (B) in Table 1.

Table 1. Equations Defining Species Allocation Model No. 1

$$\sum_{i=1}^{N} X_{i,J} = 1.0 \qquad X_{i,J} \geq 0 \tag{A}$$

$$TTM_J = \frac{\sum_{i=a}^{b} \ln \dfrac{X_{i,J}X_{KS,JR}}{X_{i,JR}X_{KS,J}}}{\sum_{i=a}^{b} \ln (\alpha_{i,KS})} \tag{B}$$

$$J < N \begin{cases} a = 1 \\ b = KS \end{cases}$$

$$J > N \begin{cases} a = KS \\ b = N \end{cases}$$

$$X_{i,J} = X_{i,JR} \frac{X_{KS,J}}{X_{KS,JR}} \alpha_{i,KS}{}^{TTM_J} \tag{C}$$

$$\alpha_{i,KS} = SQRT(\alpha^J{}_{i,KS} \cdot \alpha^{JR}{}_{i,KS}) \tag{D}$$

$$\alpha^J{}_{i,KS} = K_i{}^J / K^J{}_{KS} \tag{E}$$

$$J < N \begin{cases} JR = KS = N + 1 - I \\ J = N - I \end{cases} \qquad I = 1, 2, , , , N - 1$$

$$J > N \begin{cases} JR = N - 1 + I \\ KS = I \\ J = N + I \end{cases} \qquad I = 1, 2, , , , N - 1$$

Table 2. SAC Array Derived from SAM 1

J	TTM_J	T_J(°K)	$X_{1,J}$	$X_{2,J}$	$X_{3,J}$
1	2.12	309.96	0.98988	0.01000	1.19-4
2	2.12	311.48	0.89891	0.09110	0.01000
3	0.00	331.65	0.33300	0.33400	0.33300
4	2.37	365.91	0.01000	0.09920	0.89081
5	2.62	371.15	8.25-5	0.01000	0.98992

Table 3. SAC Array Derived from SAM 2

J	$X_{1,J}$	$X_{2,J}$	$X_{3,J}$	$X_{4,J}$	$X_{5,J}$
1		1.-2	1.-4	1.-6	1.-8
2			1.-2	1.-4	1.-6
3				1.-2	1.-4
4					1.-2
5					
6	1.-2				
7	1.-4	1.-2			
8	1.-6	1.-4	1.-2		
9	1.-8	1.-6	1.-4	1.-2	

Table 4. Transpose of Final Product Composition Array Derived from SAM 1

J	$X_{1,J}$	$X_{2,J}$	$X_{3,J}$
1	0.98980	0.0100	1.19-4
2	0.01000	0.9800	0.01000
3	8.3-5.0	0.0100	0.98992

Table 5. Transpose of Final Product Composition Array Derived from SAM 2

J	$X_{1,J}$	$X_{2,J}$	$X_{3,J}$	$X_{4,J}$	$X_{5,J}$
1	0.989	1.-2	1.-4	1.-6	1.-8
2	1.-2	0.979	1.-2	1.-4	1.-6
3	1.-4	1.-2	0.979	1.-2	1.-4
4	1.-6	1.-4	1.-2	0.979	1.-2
5	1.-8	1.-6	1.-4	1.-2	0.989

Let each of these trays have a component KS whose composition is specified equal to a purity specification for the final products. (In this study, the specification was 0.01.) The defining relationships for the subscript KS are given in Table 1. The purity of the products can be varied from one final product to the next. (This specification determined the values obtained for the concentrations with asterisks in Table 4 of Part I.)

The first tray $N - 1$ above the feed tray N is separated from its reference tray N by TTM_{N-1} minimum theoretical stages as defined by Equation (B) in Table 1. The second such tray is separated from tray $N - 1$ by TTM_{N-2} theoretical stages and has tray $N - 1$ for its reference tray. By trial and error, a set of concentrations for all trays and a minimum number of theoretical stages separating each of these trays can be found which satisfy the relationships shown. After convergence, the rows in this SAC array are used to synthesize the final product composition array.

An example SAC array produced by this model is shown in Table 2. The relative volatilities used in the model are considered a function of the bubble-point temperature, except for the top row where they are treated as a function of the dew point. These temperatures are usually evaluated at an assumed total pressure of 1 atm. They are shown in Table 2 along with the minimum theoretical stages.

The second species allocation model (SAM 2) examined is more heuristic than the first, having no theoretical basis like the Fenske equation. It is used to define elements of the SAC array with Equations (1) and (2) as defined below:

$$X_{i,J} = XS^{i-j} \quad J < N, \quad i > J \tag{1}$$

$$X_{i,j} = XS^{J+1-N-i} \quad J > N, \quad i < J + 1 - N \tag{2}$$

where XS is a purity specification like 0.01. This model is simpler than SAM 1 since it requires no trial and error calculations. Table 3 shows how these equations are applied to give the incomplete SAC array for a five-component example. The unspecified composition elements in rows 1 and 9 are obtained by difference and Equation (A) in Table 1.

The SAC array generated from either SAM 1 or SAM 2 is used to synthesize the final product composition array $\underline{\mathbf{XP}}$ which has dimensions N by N. The composition of the lightest stream is taken directly from row 1, columns 1 through N, of the SAC array. The composition of the heaviest product stream is also taken directly from the bottom row, columns 1 through N, of the SAC array. Product streams between the lightest and heaviest have two keys and two component purity specifications rather than one. For final product streams P_J, $J = 2, 3, , , N - 1$, the components $J - 1$ and $J + 1$ are the light and heavy keys, respectively. The concentrations of components 1 through $J - 1$ in product J are estimated by using the composition values in columns 1 through $J - 1$ of row $N + J - 1$ of the SAC array. The concentrations of components $J + 1$ through N for the same product J are estimated from the values in columns $J + 1$ through N of row J of the SAC array. The concentration of the J^{th} component is estimated by Equation (A) in Table 1.

Tables 4 and 5 show the results of synthesizing final product composition arrays using the SAC arrays in Tables 2 and 3, respectively. These product compositions are similar to what one would expect to obtain from an equilibrium-stage model. But instead of being calculated as dependent variables as for that case, the compositions are synthesized and used as torn or assumed variables in the composition node design model.

Definition of the Interconnecting Links

The original feed and final product streams define the overall separation objectives. Intermediate product streams are also feed streams connecting subproblems. These stream vectors are calculated using the overall steady state material balances. Given the original feed rate column vector, $\mathbf{FX}$, the molar rate of each component in the original feed, the final product column vector $\mathbf{P}$ is estimated from the overall steady state material balances using the final product composition array synthesized from the SAC array:

$$\mathbf{P} = \underline{\mathbf{XP}}^{-1}\mathbf{FX} \tag{3}$$

Once the overall product rates are calculated for the separation system, then the material balance equations are used to define a set of $N(N - 1)/2$ mass rates and feed compositions which are used as interconnecting links between the towers. The compositions are also used to define the external vertexes in the respective towers. Feed rates are obtained by summing over the product streams

$$F_j(I, J) = \sum_{k=I}^{J} P_K \quad J > I \tag{4}$$

where the feed rate $F_j(I, J)$ yields final products I through J. Similarly, the feed concentrations are obtained by the component balances

$$XF_{i,j}(I, J) = \frac{\sum_{k=I}^{J} XP_{i,k}P_k}{F_j(I,J)} \quad J > I \tag{5}$$

where the i^{th} component rate in the j^{th} feed is obtained by summing the i^{th} row of $\underline{\mathbf{XP}}$ from columns I to J.

Equations (3) through (5) have been used to gen-

Table 6. Interconnecting Mass Rates and Stream Compositions Derived from SAM 1

Product	P_J	$XP_{1,J}$	$XP_{2,J}$	$XP_{3,J}$
1	233.10	0.9898	0.0100	1.19-4
2	233.81	0.0100	0.9800	0.0100
3	233.08	8.25-5	0.0100	0.9899
Feed	F_J	$XF_{1,J}$	$XF_{2,J}$	$XP_{3,J}$
1	700.00	0.3330	0.3340	0.3330
2	466.92	0.4992	0.4957	0.0051
3	466.90	0.0050	0.4958	0.4992

erate Table 6 from the final product composition array shown in Table 4. Feed 1 in Table 6 is the original feed. Feed 2 is producing products 1 and 2, while feed 3 is producing products 2 and 3.

Composition Node Definitions for Designs I through VIII

The species allocation defines feed and product streams connecting the towers. The manner in which this assignment is made is shown in Figure 1. In this figure are shown the graph representations for designs I through VIII (see Part I). Each node in the graphs is labeled either with a *P*, *F*, *IP*, or *ID* designation. The *P* and *F* designations correspond to the product and feed labels in Table 6. Counting the vertexes in each design from left to right and top to bottom, node one in each design is labeled *F*1 which corresponds to the original feed. The labels *P*1, *P*2, and *P*3 appear in each graph and indicate the location at which products 1 through 3 are removed from the system.

In design III nodes 4 and 7 are both labeled with *F*3. Similarly, in design IV nodes 3 and 6 are both designated as *F*2. The towers in both designs are thermally coupled at those locations as indicated by the double arrows connecting the respective vertexes. Node 7 in design III is assumed to have the same composition as node 4. Similarly, node 6 is assigned the same composition as 3 in design IV. Both of these assignments are based on a nonenrichment assumption. Obviously, this assumption isn't true, as enrichment will occur between those locations. The assumption is acceptable for design purposes, however, as it leads to systematic overdesign.

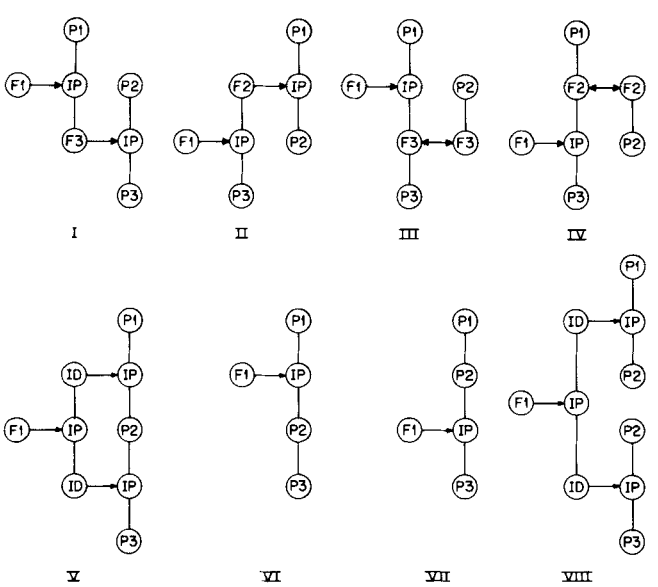

Fig. 1. The composition node definitions for designs I through VIII (see Part I).

The *IP* and *ID* designations refer to nodes whose compositions are internal and cannot be defined by the SAM since they must vary during the state optimization. The *IP* label refers to feed trays whose composition varies with the feed fractional vaporization, an optimization variable. The *ID* designation identifies a composition node which varies during the state optimization when the fraction of the feed sent overhead is an optimization variable. These nodes represent locations in the design where components are distributed between the keys. Notice that this designation only occurs for the upstream towers of designs V and VIII. An explanation of the calculational procedures for these two types of internal nodes is left to the appendixes where the PINCH and DISTRIB algorithms are described.

Composition Node Design Method

By species allocation, the tower overall material balances are heuristically established before the state optimization is begun. Because the vertex compositions are torn in a realistic manner, the remaining calculations are greatly simplified without gross distortion of the design model.

A tower receiving *NF* feeds is defined by $R - NF$ tower vertexes (the primitive system) which are numbered starting with the overhead vertex $NF + 1$. The vertexes 1 through *NF* define feed streams. Among the tower vertexes, $R - 2NF$ of them are defined either by the species allocation or the DISTRIB algorithm. The remaining *NF* vertexes represent tower feed trays whose compositions are estimated by the PINCH algorithm.

The pressure profile for the tower is defined by the optimization routine which specifies the overhead total pressure and the pressure drop per section. At this point in the calculations, the bubble- and dew-point temperatures for all tower vertexes can be estimated since the compositions are also known. From them, the vapor enthalpy vector and the liquid enthalpy vector for the tower can also be established:

$$\mathbf{H}_v = \mathbf{H}_v(\underline{\mathbf{X}}_R, \mathbf{T}_d) \tag{6}$$

$$\mathbf{h}_L = \mathbf{h}_L(\underline{\mathbf{X}}_R, \mathbf{T}_b) \tag{7}$$

$$\underline{\mathbf{E}} = \mathbf{H}_v \; U \; \mathbf{h}_L \tag{8}$$

$$\dim(\underline{\mathbf{X}}_R) = (R - NF) \times N$$

$$\dim(\mathbf{T}_d) = \dim(\mathbf{T}_b) = (R - NF)$$

$$\dim(\underline{\mathbf{E}}) = (R - NF) \times 2$$

The Underwood Equations

The overflow and vapor rates within the tower must change during the state optimization. The vapor rate at the pinch point for the tower is determined from the state variables specified by the optimization routine and using the Underwood equations. For a tower receiving a vector of *NF* feeds and specified fractional vaporization, there exists a vector of $N - 1$ roots, each of which satisfies the scalar equation

$$Q_1(\lambda_k) = \mathbf{F}^T(\mathbf{f} - \underline{\mathbf{X}}_F\boldsymbol{\delta}_k) = 0 \tag{9}$$

$$\boldsymbol{\delta}_k{}^T = [\alpha_1/(\alpha_1 - \lambda_k), \ldots \alpha_N/(\alpha_N - \lambda_k)] \tag{10}$$

$$k = 1, 2, \ldots N - 1$$

$$\dim(\mathbf{F}) = NF = \dim(\mathbf{f})$$

$$\dim(\underline{\mathbf{X}}_F) = NF \times N$$

Each row in $\underline{\mathbf{X}}_F$ is the composition of one feed.

For a tower receiving a single feed, Equation (9) reduces to the more familiar form

$$Q_2(\lambda_k) = f - \mathbf{X}_F\boldsymbol{\delta}_k = 0 \qquad (11)$$

where $\mathbf{X}_F$ is a row vector with dimension N.

Now, the Underwood Equations (9) and (11) assume constant relative volatility. When a tower receives a single feed, Equation (11) leads to roots $\boldsymbol{\lambda}$ which are used to calculate the minimum vapor rate. Lockhart (1947) and Robinson and Gilliland (1950) point out, however, that the method tends to be conservative. This observation is confirmed here.

When a tower receives multiple feeds, the constant relative volatility assumptions needed in Equation (9) become even less valid because the tower contains more sections and the temperature drop up the tower is larger. This has the effective result of increasing the degree of overdesign. An alternative procedure for towers with multiple feeds is to apply Equation (11) to each feed tray individually to obtain a local root vector $\boldsymbol{\lambda}_j$. The local root vector is then used to calculate the minimum vapor rates for those tower sections adjacent to the feed. This latter method results in less overdesign.

Consider example B described below. This example is for the downstream tower in design V, where a tower receives two feeds. The latter method described above was used to design this tower. On that basis, a minimum vapor rate of 0.091 kg-mole/s was calculated. Equivalent analysis with an equilibrium-stage model indicates that the vapor rates for that tower are about right. The application of Equation (9) to the same tower gives an estimated minimum vapor rate of 0.128 kg-mole/s. Thus, this equation, a rigorous application of the Underwood method, leads to an estimate of the minimum vapor rate for the downstream tower which is about 40% high.

For this reason, Equation (11) was used exclusively to calculate the Underwood minimum vapor rates. The local root vectors give better estimates of the true vapor requirements since they allow the relative volatilities to be adjusted to their local values at the feed tray.

Every tower can be divided into $R - NF - 1$ sections, each of which is defined by two adjacent tower nodes. An Underwood minimum vapor rate $V^U_{r,k}$ can be defined for each section and for each of the $N - 1$ local roots calculated at the feed tray adjacent to the tower section or closest to it. The downstream tower for design V, for example, is represented by the graph shown in Figure 1. This tower contains four sections. Defining the sums, we get

$$SF_{j,k} = \sum_{i=1}^{N} XF_{i,j}\alpha_i/(\alpha_i - \lambda_k) \qquad (12)$$

$$SP_{j,k} = \sum_{i=1}^{N} XP_{k,j}\alpha_i/(\alpha_i - \lambda_k) \qquad (13)$$

where $(XF_{i,j},\ i = 1, 2, \ldots N)$ are the feed compositions for the j^{th} feed and $(XP_{i,j}\ i = 1, 2, \ldots N)$ are the compositions on the j^{th} product tray. The root vectors $\boldsymbol{\lambda}_2$ and $\boldsymbol{\lambda}_4$ are defined for the feeds entering the tower. The subscripts are according to the five vertexes in the downstream tower, numbered from top to bottom. With these conventions, the Underwood minimum vapor rates for the four tower sections are defined by the set of equations given below:

$$V^U_{2,k} = P_1SP_{1,k} \qquad (14)$$

$$V^U_{3,k} = P_1SP_{1,k} - F_2SF_{2,k} \qquad (15)$$

$$V^U_{4,k} = P_1SP_{1,k} + P_3SP_{3,k} - F_2SF_{2,k} \qquad (16)$$

$$V^U_{5,k} = V^U_{4,k} - F_4SF_{4,k} = -P_5SP_{5,k} \qquad (17)$$

If either $V^U_{2,k}$ or $V^U_{4,k}$ control, then the pinch is located either directly above the first or second feed to the tower. If either $V^U_{3,k}$ or $V^U_{5,k}$ control, then the pinch is below one of the two feeds.

Suppose that λ_{KP} is the root which controls the minimum vapor and that the pinch point is located in section RP. The vapor rate at the pinch point is then defined by

$$V^* = \theta V^U_{RP,KP} \qquad (18)$$

where θ is the ratio of vapor to minimum vapor at the pinch point which is specified as an optimization variable.

Consider the conventional countercurrent equilibrium-stage model. The steady state energy balances around a section of trays with no intermediate feeds or draws is given by

$$H_1V_1 + h_{j-1}L_{j-1} = h_0L_0 + H_jV_j \qquad (19)$$

If a single overhead product P_1 is produced, then the overall material balances give

$$V_j - L_{j-1} = P_1 \qquad (20)$$

$$V_1 - L_0 = P_1 \qquad (21)$$

Equations (19) through (21) can be combined to give

$$V_1 = V_j\left[\frac{H_j - h_{j-1}}{H_1 - h_0}\right] + P_1\left[\frac{h_{j-1} - h_0}{H_1 - h_0}\right] \qquad (22)$$

Thus, the vapor at tray 1 in the equilibrium stage model can be expressed in terms of the overhead rate P_1, the vapor rate at the j^{th} tray, and the vapor and overflow enthalpies at two sets of adjacent trays.

Using the composition node design method, however, only two trays are defined for each section of trays, not four as in (22). In this case, the section would be defined in terms of trays 1 and j. So, the approximation is made that the enthalpies of the overflow liquids are nearly the same in adjacent trays. In this case

$$h_1 \simeq h_0 \qquad (23)$$

$$h_{j-1} \simeq h_j \qquad (24)$$

Further, defining the vector $\mathbf{S}$ as the union of the feed and product vectors for a tower, we get

$$\mathbf{S} = \mathbf{F}\ U\ \mathbf{P} \qquad (25)$$

$$\dim(\mathbf{S}) = NF + NP = R - NF$$

Then, if the location of V^* is known, $R - NF$ vapor rates $\mathbf{V}$ can be defined in terms of V^*, $\mathbf{S}$, and the enthalpy array $\underline{\mathbf{E}}$ defined by Equation (8). Similarly, the overflow vector $\mathbf{L}$ can be defined from $\mathbf{V}$ and $\mathbf{S}$ with one overflow rate for each node:

$$\mathbf{V} = \mathbf{T}_{RP}(\underline{\mathbf{E}}, \mathbf{S}, V^*) \qquad (26)$$

$$\mathbf{L} = \mathbf{G}_{RP}(\mathbf{V}, \mathbf{S}) \qquad (27)$$

Here $\mathbf{T}_{RP}$ and $\mathbf{G}_{RP}$ are vector sets of equations similar in form to Equations (20) through (22). They are subscripted by RP, the section in which the pinch occurs, because they are a function of that location. The algorithm shown in Figure 2 can now be used to find the overflow and vapor profiles for any arbitrary CNDM.

Initially, V^* is assumed equal to the largest value calculated from the Underwood equations using local roots where appropriate. If the solution to Equations (26) and (27) leads to a vapor rate for any section which is less than that amount by which the vapor rate must exceed the minimum rate at the pinch point, then that section is assumed to be the pinch section. Since the same enthalpies are used to generate the new profiles, the values in the latter case will be greater than in the former. In this way,

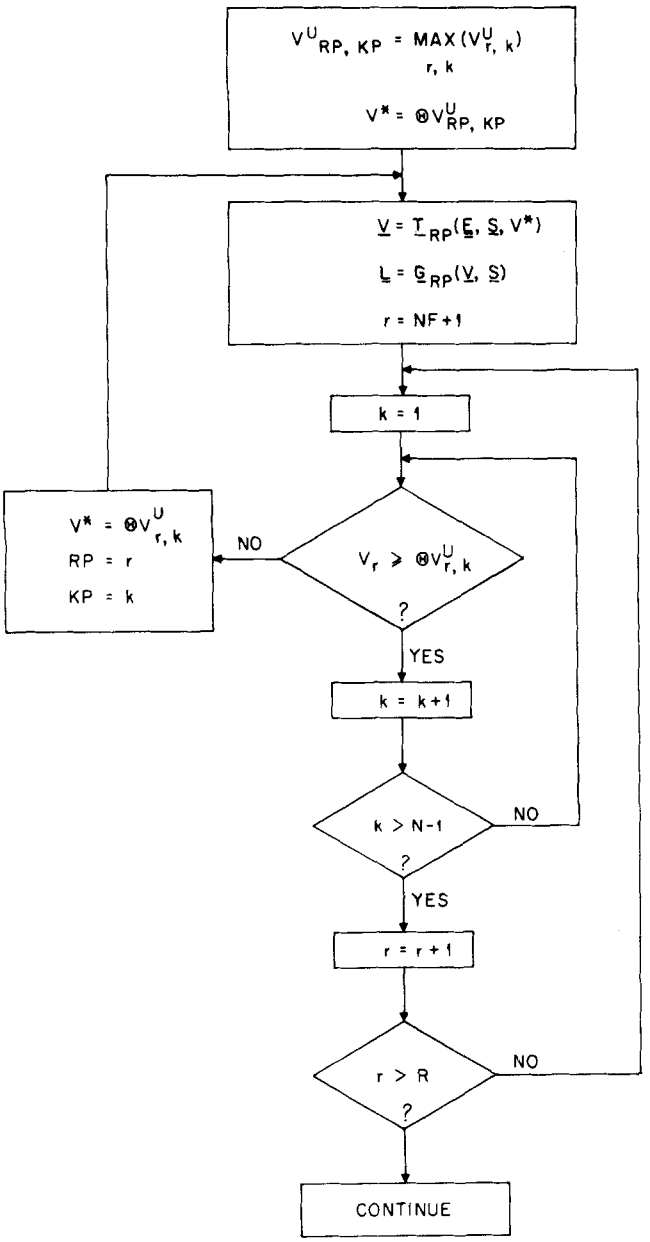

Fig. 2. Algorithm for identifying the pinch point in a tower and defining the vapor and liquid overflow profiles.

the pinch point will always be correctly identified regardless of how many sections are present or how many feeds enter the tower.

Estimating the Minimum and Actual Number of Trays

In order to estimate the minimum theoretical stages for any section, the Fenske equation is applied to all possible component pairs. This approach differs from the classical method where the light and heavy keys are always used to define the minimum theoretical trays. This method is used, however, because the compositions are torn variables. The largest value calculated from examining all possible component pairs is used to design the section. Since this procedure is repeated for each section, different pairs can control the minimum theoretical tray requirements for each section. The minimum theoretical trays for the tower are obtained by adding those trays obtained for the $R - NF - 1$ section.

MODEL EVALUATION

The CNDM leads to system models with overspecified material balances when more than two components are present in the feed. The equilibrium relationships are only approximately satisfied, but the assumptions implicit in the method are justified by the resulting computational savings and the enhanced ability to easily consider much larger classes of designs.

The modeling bias may be divided into two categories. The first category is that bias attributable to the physical properties calculations. This bias, however, is common to both the design and equilibrium stage models and is not examined here.

The second category is that bias which is due to the design method. It is examined here by assuming a set of material balances and then designing a tower with the composition node method. The bias is then estimated by simulating the same tower as an equilibrium stage model.

Comparison of the two models gives information regarding differences in state variables such as composition, overflow, and temperature at various points in the tower as well as reboiler and condenser duties. The observed differences will not necessarily be significant. For design purposes, it is only necessary that the assumed product purity specifications, for example, bound those which are actually achieved. In particular, the equilibrium-stage model should meet or exceed the assumed purities.

The equilibrium-stage model used the Thiele-Geddes method. A description of the model is given by Newman (1967). In order to simulate a tower, the following information is specified from the design model:

1. Number of theoretical trays.
2. Location of feed and product trays.
3. Total enthalpy and feed component rates.
4. Product draw rates (except overhead product).
5. Overflow rate onto the top stage L_0.

The theoretical stages used were the nearest integer to that real number obtained from the design model. The top stage overflow rate, item 5, was obtained directly from the design model print-out. It is optimized upon in the design model but remains fixed in the equilibrium-stage model. All of the other overflow rates in the tower are found by trial and error.

Eight towers have been compared using the design and equilibrium-stage models. Table 7 presents some of the tower specifications such as feed composition, product rates, and design modeled. The feed numbered 1 consists of *n*-pentane, *n*-hexane, and *n*-heptane. Feed 4 is a mixture of *i*-pentane, *n*-pentane, and *n*-hexane. Examples D through F are for a six-component feed consisting of *I*-butane, *N*-butane, *I*-pentane, *N*-pentane, *N*-hexane, and *N*-heptane. Examples G and H separate a feed consisting of propane, *i*-butane, and *n*-butane.

The results obtained from the two models are compared in Table 8, 9, and 10. The *J* subscript refers to the theoretical stage whose state is presented. The stages shown are either feed or product trays, since these are the vertexes defined in the design model. Example B shows five nodes or trays which are, starting from the top, the overhead product, upper feed, middle product, lower feed, and bottom product trays. All other examples, except H, have only three nodes presented which correspond to the overhead, feed, and bottom trays, respectively. Example H has only two nodes corresponding to conditions at the top and bottom of the downstream tower.

Examples A through C in Table 8 are for three-component systems. The agreement between the species allocation and equilibrium-stage model is good. The purity specifications for these cases are based on SAM 1, as can be seen by noting the contaminant concentrations in the product streams (that is, 0.01). The assumed purity specifications are met or exceeded for all products except the

TABLE 7. SOME OF THE TOWER SPECIFICATIONS FOR THE EIGHT EXAMPLES

Example	Product rates: Overhead	Middle	Bottom	Feed No.	Design	Tower	Feed composition
A	463.26	0.00	236.74	1	V	1	(0.1, 0.8, 0.1)
B	64.95	570.10	64.95	1	V	2	(0.146, 0.844, 0.010) (0.010, 0.714, 0.276)
C	232.30	0.00	467.70	4	I	1	(0.333, 0.334, 0.333)
D	349.32	0.00	350.68	7	—	—	(0.166, 0.167, 0.167, 0.167, 0.167, 0.166)
E	350.00	0.00	350.00	7	—	—	(0.166, 0.167, 0.167, 0.167, 0.167, 0.166)
F	350.00	0.00	350.00	7	—	—	(0.166, 0.167, 0.167, 0.167, 0.167, 0.166)
G	567.10	240.82	67.96	6	III	1	(0.8, 0.1, 0.1)
H	64.95	0.00	175.87	6	III	2	(0.005, 0.484, 0.511)

overhead product in example B. It appears that a few more theoretical stages are needed in the uppermost section of this tower to complete the separation. The overdesign for these three cases appears small. In example C, the overhead product exceeds purity specifications by the widest margin, but only 0.8%.

The overflow and temperature profiles also appear to agree surprisingly well. (The overflow rates are specified equal at the overhead stages.) Even for example B, where the changes in overflow rates are substantial, the greatest error at tray 32 is less than 7%.

The largest errors occur at the feed trays. This inadequacy exists partly because the feed line equation alone, as it is used in the PINCH algorithm, is not sufficient to give a good estimate of the feed tray composition. In particular, this equation does not take the adjacent vapor and overflow streams into account. Consequently, the composition on the feed tray approximates the feed composition too closely. This error leads to differences in the enthalpy estimates at that location and therefore the overflow rates at the product trays. The vapor rate at the feed tray is not affected by this shortcoming when it is calculated from the Underwood equations and the vapor to minimum vapor ratio. But it does affect the vapor calculations for the tower overhead and bottoms. Since the overflow rates at the feed trays are low, the design model appears to overestimate the required overflows at product trays.

The tower diameter is normally based on the volumetric flow rate at the overhead tray where the total pressure is the least and the molar vapor rate normally appears the greatest. Consequently, the overflow bias due to the composition errors at the feed tray may tend to overestimate the required tower diameter.

The agreement in condenser and reboiler duties is surprisingly good. In example C, the bottoms overflow rate is roughly triple that in example A. Yet the duty error is

TABLE 8. COMPARISON OF SPECIES ALLOCATION AND EQUILIBRIUM-STAGE MODELS FOR EXAMPLES A, B, AND C

	SAM and CNDM					Equilibrium stages				
J	T_J	AL_J	$X_{1,J}$	$X_{2,J}$	$X_{3,J}$	T_J	AL_J	$X_{1,J}$	$X_{2,J}$	$X_{3,J}$
				Example A						
1	360	361	0.146	0.844	0.010	360	361	0.151	0.841	0.008
8	367	321	0.100	0.800	0.100	370	345	0.049	0.859	0.097
15	378	1 031	0.010	0.714	0.276	380	1 032	0.3-03	0.694	0.306
	Condenser duty			2.2534 + 10		2.2786 + 10		−1.11% error		
	Reboiler duty			2.3988 + 10		2.3869 + 10		+0.50% error		
				Example B						
1	328	411	0.990	0.010	0.2-05	328	411	0.978	0.022	0.4-09
15	358	343	0.143	0.847	0.010	360	356	0.117	0.877	0.006
22	367	830	0.010	0.980	0.010	367	822	0.011	0.980	0.009
32	377	221	0.007	0.690	0.303	377	236	0.9-04	0.698	0.301
46	404	436	0.1-05	0.010	0.990	404	420	0.7-11	0.004	0.996
	Condenser duty			1.1751 + 10		1.1814 + 10		−0.53% error		
	Reboiler duty			1.0497 + 10		1.0440 + 10		+0.54% error		
				Example C						
1	327	2 286	0.990	0.010	0.6-10	327	2 286	0.998	0.002	0.2-22
45	341	1 982	0.365	0.342	0.293	335	2 179	0.464	0.426	0.110
88	353	2 820	0.007	0.495	0.498	353	2 802	0.003	0.498	0.499
	Condenser duty			5.8231 + 10		5.8222 + 10		+0.02% error		
	Reboiler duty			6.2760 + 10		6.2186 + 10		+0.92% error		

Units

AL_J	overflow onto J^{th} tray	kg-mole/hr
T_J	temperature on J^{th} tray	°K
	All duties	J/hr

Table 9. Comparison of Species Allocation and Equilibrium-Stage Models for Examples D, E, and F

		SAM and CNDM							Equilibrium stages							
J	T_J	AL_J	$X_{1,J}$	$X_{2,J}$	$X_{3,J}$	$X_{4,J}$	$X_{5,J}$	$X_{6,J}$	T_J	AL_J	$X_{1,J}$	$X_{2,J}$	$X_{3,J}$	$X_{4,J}$	$X_{5,J}$	$X_{6,J}$
		Example D														
1	312	1 372	0.332	0.334	0.329	0.005	0.2-04	0.8-05	312	1 372	0.333	0.335	0.332	0.9-03	0.3-20	0.1-36
40	327	905	0.235	0.194	0.153	0.148	0.138	0.134	345	1 213	0.031	0.049	0.479	0.299	0.079	0.063
84	380	1 912	0.5-03	0.9-03	0.005	0.329	0.333	0.332	381	1 901	0.6-24	0.4-18	0.003	0.332	0.333	0.331
		Condenser duty			3.7539 + 10					3.7507 + 10		+0.09% error				
		Reboiler duty			4.5404 + 10					4.439 + 10		+2.27% error				
		Example E														
1	313	339	0.327	0.324	0.195	0.140	0.010	0.004	313	339	0.332	0.334	0.215	0.118	0.9-03	0.3-05
7	335	129	0.160	0.164	0.168	0.169	0.170	0.170	345	255	0.072	0.105	0.252	0.246	0.175	0.150
15	376	930	0.005	0.010	0.139	0.194	0.324	0.328	379	893	0.3-04	0.3-03	0.119	0.216	0.333	0.332
		Condenser duty			1.5666 + 10					1.5284 + 10		+2.50% error				
		Reboiler duty			1.7202 + 10					1.5934 + 10		+7.95% error				
		Example F														
1	314	228	0.322	0.256	0.199	0.169	0.043	0.010	312	228	0.332	0.334	0.200	0.122	0.011	0.7-03
4	333	76	0.166	0.167	0.167	0.167	0.167	0.166	340	168	0.084	0.123	0.237	0.214	0.180	0.162
19	365	842	0.010	0.077	0.135	0.165	0.291	0.322	377	832	0.7-07	0.6-05	0.134	0.212	0.323	0.331
		Condenser duty			1.3909 + 10					1.3053 + 10		+6.56% error				
		Reboiler duty			1.5247 + 10					1.4111 + 10		+8.05% error				

essentially zero in both cases. The duty errors, therefore, are not a strong function of the vapor rate in the tower.

Examples D through F in Table 9 are for a six-component feed whose species are fed to the towers in nearly equimolar amounts. Example D is for a sharp split, namely ABC/DEF. SAM 1 was used to estimate the material balances, and agreement with the equilibrium-stage model appears adequate. Again, the largest discrepancies appear to revolve around the feed tray composition. Although a 25% error in overflow rate occurs at the feed tray, the discrepancy is less than −1% at the overflow onto the bottom tray. This overflow error at the bottoms in example D, combined with a small temperature difference at that point, leads to a +2.27% error in reboiler duty for the tower. The error is slightly larger than for examples A through C, but still acceptable as overdesign. The purities achieved by the equilibrium-stage model suggest, again, that overdesign has been committed, but the differences are acceptably small for the light and heavy keys, namely, components 4 and 3 in this case.

Examples E and F also utilize SAM 1 and the normalization procedure described in DISTRIB for the design models. Example E is for the ABCD/CDEF split so that components C and D are distributed. Example F shows the ABCDE/BCDEF split where components B through E are distributed. The overdesign for these cases still appears reasonable from the purity standpoint.

The duty errors increase to a maximum of 8% overdesign for the reboiler in example F. They are seen to increase going from example D to F although the overflow rates for example F are substantially less than for D. This comparison shows clearly that the duty error magnitudes depend not on the tower size or vapor rates, but rather on the nature of the split. Thus, the errors associated with a tower performing a sharp split will generally be less than those for one performing a split with distributed components. Consequently, the duty errors in example F should represent an upper bound on those which would be expected for the simple towers designed to separate feed 7, since all the remaining towers generate fewer distributed components.

Table 10. Comparison of Species Allocation and Equilibrium-Stage Models for Examples G and H

		SAM and CNDM				Equilibrium stages				
J	T_J	AL_J	$X_{1,J}$	$X_{2,J}$	$X_{3,J}$	T_J	AL_J	$X_{1,J}$	$X_{2,J}$	$X_{3,J}$
		Example G								
1	315	415	0.986	0.010	0.004	315	415	0.987	0.011	0.001
9	319	335	0.861	0.072	0.068	319	378	0.846	0.101	0.053
32	363	1 695	0.005	0.484	0.511	358	1 727	0.2-06	0.813	0.187
78	371	1 684	0.7-06	0.010	0.990	371	1 682	0.2-24	0.5-3	0.999
		Condenser duty = 1.3113 + 10				Condenser duty = 1.3097 + 10			+0.12% error	
		Reboiler duty = 2.4372 + 10				Reboiler duty = 2.4352 + 10			+0.08% error	
		Example H								
1	355	189	0.010	0.980	0.010	356	189	0.1-05	0.968	0.032
45	362	176	0.005	0.484	0.511	358	187	0.2-06	0.810	0.190
		Condenser duty = 3.6916 + 09				Condenser duty = 3.6901 + 09			+0.04% error	
		Reboiler duty = 0.0				Reboiler duty = 9.2995 + 06			+0.04% error*	

* Percentage of total reboiler duty.

In example F, SAM 1 and SAM 2 give the same material balances since there are no contaminants and the key concentrations are specified in either case. In example E, however, SAM 2 gives slightly different compositions for component 6 in the overhead and 1 in the bottoms. From the material balance standpoint, these differences are negligible, and the overflow and temperature profiles for SAM 1 and SAM 2 are nearly the same at the optimal states. In both cases, a 1.68 m diameter tower is required ($\pm$ 0.03 m). Thus, changing the species allocation model does not have a significant effect on this important tower parameter, since the minimum vapor rates depend primarily on the principal components in a product stream and not on the contaminants.

SAM 2, however, leads to gross overestimation of the minimum theoretical trays for example E. This unacceptable overdesign occurs as follows. For SAM 1, the minimum theoretical trays are determined by the component pair (4, 5) for the upper section and by the pair (2, 3) for the lower. This control is normal for a tower performing the ABCD/CDEF split. When SAM 2 is used, the height of the upper section is controlled by the component pair (5, 6) and by pair (1, 2) for the lower. This control is abnormal and leads to gross overdesign. Instead of requiring 5.84 minimum theoretical trays, the latter model estimates that 20.14 trays are required. Thus, instead of building a tower 19 m high, SAM 2 estimates that a tower height of 45 m is needed. Clearly, this difference is unacceptable and shows a significant weakness in the latter species allocation method, namely, that use of SAM 2 can lead to significant overestimation of the tower height.

But SAM 2 is still useful so long as the component pairs defining the minimum theoretical trays in the tower sections are normal for the stated tower objectives. If control is abnormal, then the assumed contaminant concentrations can be adjusted upward so as to yield normal control. SAM 1 is less likely to result in this type of error since the minimum theoretical trays for all adjacent pairs tend to be numerically close to each other. Consequently, even when abnormal control is observed with SAM 1, the discrepancies in tower heights appear insignificant.

Examples G and H in Table 10 compare the CNDM with an equivalent, equilibrium-stage model of design III, consisting of two thermally coupled towers (see Part I). This design is particularly important because it was found substantially less expensive to separate a feed consisting of 80% propane from equal amounts of iso and normal butanes using this design III, rather than the expected optimal design I. So this example represents a case where thermal coupling significantly reduces the downstream tower size and vapor requirements, and the total design costs.

If we examine Table 10, the stages identified with the J subscript have the following significance. Example G describes the upstream tower which takes the propane product from stage 1, receives the external feed (80% propane) at stage 9, is thermally coupled at stage 32, and produces a bottom product at stage 78. In example H, the downstream tower produces a middle product at stage 1 and is thermally coupled with the upstream tower at stage 45.

Using the SAM and CNDM, the composition of the overflow liquids are defined as being equal at the point of thermal coupling between the towers, consistent with the no enrichment assumption (also see Figure 1). Consequently, the compositions at stage 32 in example G and at stage 45 in example H are exactly equal in the design model. However, the compositions at these two points are different using the equilibrium-stage model, since enrichment does occur. When we compare the compositions at stage 32 in example G for the CNDM and equilibrium-stage models, the important point is that the CNDM underestimates the concentration of middle product at that point and overestimates the concentrations of overheads and bottom products. Similarly, at stage 45 in example H, the bias in the design model is similar, and causes some overdesign.

Estimation of the material and energy balances for this design configuration is relatively simple using the CNDM and SAM 1. Seventy cost evaluations were completed on a UNIVAC 1110 in about 7 s of CPU time. Each evaluation required complete restimation of all material overflow profiles and energy duties for both towers.

However, the equivalent, equilibrium-stage model is more complicated, since iterative calculations are required to estimate enthalpy and molar feed rates for the two towers at the point of thermal coupling, as well as converging on the energy and material balances for each tower sequentially. Using the Thiele-Geddes method, all feed compositions, rates, and enthalpies must be specified for each tower. So, in performing the calculations, each tower was initially assumed to receive the feed composition and enthalpy as estimated from the design model at the point of thermal coupling. After each tower was converged for the assumed feeds, the thermally coupled feed compositions and enthalpies were updated, and the calculations were repeated by successively substituting the new feed estimates.

Using the Thiele-Geddes method, the condenser and reboiler duties are obtained for both towers as dependent variables. Whenever the towers are not exactly thermally coupled, a nonzero reboiler duty is calculated for the downstream tower. In the CNDM, the downstream tower reboiler duty is zero by definition. On the first iteration with the equilibrium-stage model, the calculated reboiler duty for the downstream tower was about 0.69% of the estimated duty for the upstream reboiler, using the feed estimates for both towers at the point of thermal coupling obtained from the design model print-out. This error decreased monotonically, however, as the feed estimates were improved at the point of thermal coupling. After twenty iterations between the towers (and 2.18 min of CPU time on an IBM 360/91), the calculated reboiler duty for the downstream tower was 0.04% of the estimated duty for the upstream reboiler, as shown in Table 10, example H. So, convergence between the two thermally coupled towers had not yet been achieved in the equilibrium-stage model.

If we examine the product trays in examples G and H, it appears that the two models are essentially equivalent. In example G, the equilibrium-stage model predicts that the assumed product specifications are exceeded for the overhead product at stage 1 and the bottoms product at stage 78. In example H, the equilibrium-stage model predicts that the assumed product specifications for the middle product are exceeded with respect to propane contamination but are deficient with respect to the *n*-butane contamination. However, this apparent deficiency was decreasing with each successive substitution of the thermally coupled feeds between the towers. As the reboiler duty on the downstream tower was reduced during each calculation, the overflow from stage 45 in example H and stage 32 in example G was increased. Consequently, we believe that this apparent deficiency is an artifact of incomplete convergence between the thermally coupled towers modeled as the equilibrium stages, rather than inadequacy in the design model. After the first convergence of the downstream tower, the equilibrium-stage model predicted that

he middle product would contain 22.4 mole % normal butane, so the calculations are relatively sensitive to the stripping rate in the bottom section of the upstream tower.

ACKNOWLEDGMENT

The authors wish to acknowledge the helpful consultation of Professor R. R. Hughes at the University of Wisconsin. This work was supported by the Wisconsin Alumni Research Foundation, the University of Wisconsin Graduate School and Chemical Engineering Department, the National Science Foundation, and the Oak Ridge National Laboratory, which is operated by Union Carbide Corporation for the Department of Energy.

APPENDIX A: The PINCH Algorithm

This algorithm estimates the composition on the feed tray by finding a set of compositions similar to the feed composition which satisfy the feed line equation:

$$Y_i^p = [(f-1)/f]X_i^p + Z_i^F/f \qquad \text{(A1)}$$

Also, the vapor concentrations must satisfy

$$Y_i^p = \alpha_i X_i^P/\beta \qquad \text{(A2)}$$

$$\beta = \sum_1^N \alpha_i X_i^P \qquad \text{(A3)}$$

where N components are in the mixture. The relationship

$$\sum_1^N X_i^p - 1.0 = 0 \qquad \text{(A4)}$$

must also be satisfied.

Initially, PINCH assumes that $x_i^p = Z_i^F$ for $i = 1, 2, \ldots N$. The routine then converges by successive substitution. During the process the relative volatilities α_i are updated using a bubble-point subroutine

$$T_p = \text{BUBT}(\mathbf{X}^p) \qquad \text{(A5)}$$

where the bubble point is a function of the liquid concentration vector $\mathbf{X}^p$. The total pressure at the feed trays is assumed equal to a specified constant throughout the calculations.

With these conventions, the PINCH algorithm is as shown in Figure 3.

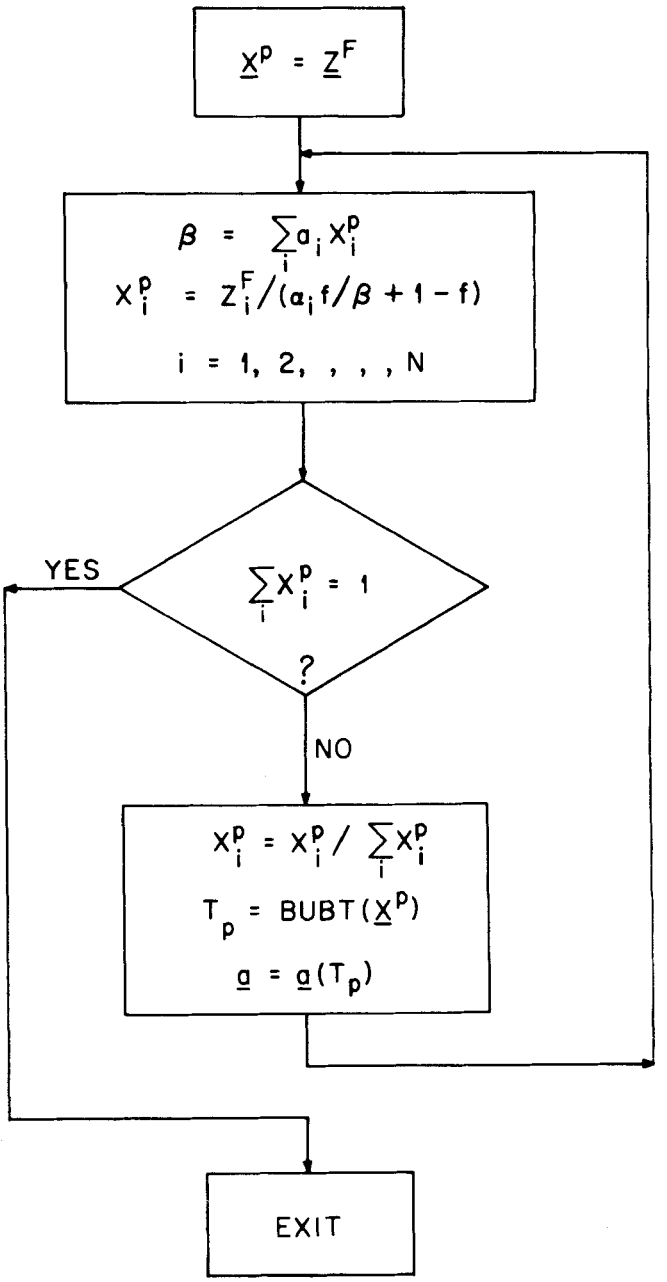

Fig. 3. The PINCH algorithm for estimating feed tray compositions.

APPENDIX B: The DISTRIB Algorithm

This algorithm is used to calculate compositions for internal vertexes labeled *ID* in Figure 1. It is only used for the upstream towers of designs V and VIII. The procedure will be described first for three-component systems.

Consider a tower producing overhead and bottom streams P_1 and P_3. The feed composition is given by $\mathbf{X}^F$. The overhead composition is $X_{i,1}$, $i = 1, 2, 3$. The bottoms composition is $X_{i,3}$, $i = 1, 2, 3$. The tower is producing the AB/BC split, so that the middle component is distributed. This means that the C concentration in the overhead product is specified as well as the A concentration in the bottoms.

Let the variable g represent the ratio of overhead to feed, that is, P_1/F. If there are purity specifications on both product streams, then the range over which g can be optimized will be a function of those purity specifications as well as the feed composition. In particular, a minimum value can be specified for g by the recovery requirements which are placed on the light component A. If g is less than the minimum g_{min}, then $X_{1,3}$ will have to increase above its specified value.

Similarly, the purity requirements placed on the heavy component will determine a maximum value for g. If g exceeds g_{max}, then more of the bottom component C will be recovered in the overhead product than is desired.

The component material balances can be used to establish values for g_{min} and g_{max}. In particular, a balance for the light component gives

$$g_{min} = (X_1{}^F - X_{1,3})/(X_{1,1} - X_{1,3}) \qquad \text{(B1)}$$

If $X_{1,3}$ and $X_{3,1}$ are both set at 0.01, then an approximate upper bound for $X_{1,1}$ is 0.99. Then, g_{min} remains a function of the feed composition.

Similarly, an upper bound on g can be established by a component balance around component C:

$$g_{max} = (X_{3,3} - X_3{}^F)/(X_{3,3} - X_{3,1}) \qquad \text{(B2)}$$

If the same purity requirements are placed on $X_{1,3}$ and $X_{3,1}$, then an upper bound for $X_{3,3}$ is given by 0.99, and with Equation (B2) g_{max} remains a function of the feed composition.

For a given value of g, the overhead rate of the bottom product $Z_{3,1}$ ($P_1X_{3,1}$) and the bottom rate of the overhead product $Z_{1,3}$ can be calculated from the purity specification. The component balances can then be used to calculate $X_{1,1}$ and $X_{3,3}$. The concentrations of the middle product $X_{2,1}$ and

$X_{2,3}$ are simply obtained by difference. Surprisingly, this simple procedure appears to give consistently good results when compared to an equilibrium stage model. Notice, however, that the equilibrium properties do not enter into the calculations of the overhead and bottom products. They are determined by feed compositions and draw rates.

When more than three components are present in the feed, the DISTRIB algorithm becomes slightly more complicated. Equations like (B1) and (B2) can still be used to calculate the feasible range for g. But now g_{min} is determined not just by the lightest component, but by that light nondistributed component which gives the largest value for g_{min} calculated for its component balance. Similarly, g_{max} is determined by that heavy nondistributed component which gives the smallest value for g_{max} calculated from its component balance.

The concentrations for the heavy nondistributed components and the light nondistributed components can be taken directly from the SAC array. When there is more than a single distributed component, however, a normalization procedure must be used to estimate their relative concentrations in the overhead and bottom products. An alternative to this normalization procedure is to use the no enrichment assumption for the distributed components.

The normalization procedure works as follows. The relative volatilities $\alpha_{i,j}$ are subscripted so that they refer to the volatility of i divided by that of component j.

The first step is to use the Fenske equation to calculate the theoretical trays separating the light and heavy keys *KL* and *KH*. Their compositions in the overhead and bottom products are known from the purity specifications they must meet and their overall component balances:

$$C = LN[(X_{KH,1}X_{KL,3})/(X_{KH,3}X_{KL,1})]/LN(\alpha_{KH,KL}) \tag{B3}$$

Here the concentration of the heavy key is specified in the bottoms and that of the light key in the overheads.

If we use the molar rates of the keys as pivot values, molar rates for the distributed components are calculated by the following equations:

$$\beta_{KH,i} = (Z_{KH,1}/Z_{KH,3})\alpha_{KH,i}^{-c} \tag{B4}$$

$$Z_{i,1} = [\beta_{KH,i}/(1 + \beta_{KH,i})]FX_i^F \tag{B5}$$

$$OD_1 = P_1 - \sum_{1}^{KH} Z_{i,1} - \sum_{KL}^{N} Z_{i,1} \tag{B6}$$

$$\text{NORM} = \sum_{K2}^{K3} Z_{i,1} \tag{B7}$$

$$Z_{i,1} = Z_{i,1}OD_1/\text{NORM} \tag{B8}$$

$$Z_{i,3} = FX_i^F - Z_{i,1} \tag{B9}$$

$$K2 = KH + 1$$

$$K3 = KL - 1$$

$$i = K2,\quad K2 + 1,\quad \ldots K3 - 1,\quad K3$$

In the above equations, (B4) is simply the Fenske equation where $\alpha_{KH,i}$ is the ratio of molar rates in the overhead and bottom products for the i^{th} component calculated using the heavy key. Equation (B5) is just a component balance based on this assumed ratio. Since, in general, the sum of the molar rates for the distributed and nondistributed components calculated in this way will not equal P_1, the concentrations of the distributed components are normalized using Equations (B6) through (B8).

In this manner, reasonable values for the distributed component concentrations can be obtained. A similar set of equations can be generated using the light key as a pivot element. Experience with these methods shows that one of the two keys will give reasonable results when used as the pivot element. Often both will.

NOTATION

- $\mathbf{f}$ = feed fractional vaporization vector
- $\mathbf{F}$ = tower feed rate vector (internal)
- $\mathbf{FX}$ = original component feed rate vector
- g = ratio of overheads product rate to feed rate
- $\mathbf{G}_{RP}$ = vector set of equations defining a tower overflow profile, assuming the pinch is at node *RP*
- $\mathbf{h}_L$ = tower liquid enthalpy vector
- $\mathbf{H}_v$ = tower vapor enthalpy vector
- *IP* = label defining an internal node where stream compositions are specified by the PINCH algorithm
- *ID* = label defining an internal node where stream compositions are specified by the DISTRIB algorithm
- *KL* = reference light key in DISTRIB algorithm
- *KH* = reference heavy key in DISTRIB algorithm
- *KP* = controlling Underwood root at the pinch point
- *KS* = reference key component in species allocation model
- $\mathbf{L}$ = tower overflow rate vector
- M_j = incidence matrix for j^{th} structural tower type
- N = number of components separated
- *NF* = number of feeds to a tower
- $\mathbf{P}$ = final product molar rate vector
- R = number of composition nodes in a design
- $\mathbf{T}_b$ = bubble-point temperature vector
- $\mathbf{T}_d$ = dew-point temperature vector
- T_p = temperature at the pinch point
- $\mathbf{T}_{RP}$ = vector set of equations defining a tower vapor profile, assuming the pinch is at node *RP*
- V^* = vapor rate at the pinch point
- V^U = Underwood minimum vapor rate
- $\mathbf{X}^P$ = mole fraction vector at pinch point
- $\mathbf{X}_R$ = composition array for the primitive system
- $\overline{\mathbf{XF}}$ = feed composition array
- $\overline{\mathbf{XP}}$ = final product composition array
- $\overline{\mathbf{XS}}$ = purity specification vector
- $\boldsymbol{\alpha}$ = relative volatility vector
- $\boldsymbol{\lambda}$ = root vector satisfying the Underwood equation
- θ = ratio of vapor rate to minimum vapor rate at the pinch point (optimization variable)

LITERATURE CITED

Lockhart, F. J., "Multi-Column Distillation of Natural Gasoline," *Petrol. Refiner*, **26**, 104 (1947).

Newman, J., "Numerical Solutions of Coupled, Ordinary Differential Equations," University of California, Lawrence Radiation Laboratory, Berkeley, *UCRL-17739* (Aug., 1967).

Ricker, N. L., and E. A. Grens II, "A Calculational Procedure for Design Problems in Multicomponent Distillation," *AIChE J.*, **20**, No. 2, 238 (Mar., 1974).

Robinson, C. S., and E. R. Gilliland, *Elements of Fractional Distillation*, 4 ed., McGraw-Hill, New York (1950).

Tedder, D. W., "The Heuristic Synthesis and Topology of Optimal Distillation Networks," Ph.D. thesis, Univ. Wisc., Madison (1975).

Manuscript received April 29, 1977; revision received and accepted December 16, 1977.